



Four Strandberg-type polyoxometalates with organophosphine centre decorated by transition metal-2,2'-bipy/H₂O complexes



Ting Lu, Shu-Li Feng, Zai-Ming Zhu*, Xiao-Jing Sang, Fang Su, Lan-Cui Zhang*

School of Chemistry and Chemical Engineering, Liaoning Normal University, Dalian 116029, PR China

ARTICLE INFO

Keywords:

Polyoxometalate
Strandberg-type
Organophosphomolybdate
Crystal structure
Catalytic property

ABSTRACT

Four inorganic-organic hybrid compounds composed of Strandberg-type organophosphomolybdate anion $[(C_6H_5PO_3)_2Mo_5O_{15}]^{4-}$ (abbreviated as $(PhP)_2Mo_5$) and transition metal (TM)-2,2'-bipy/H₂O complex units, namely $[(TM(H_2O)(bipy))_2(C_6H_5PO_3)_2Mo_5O_{15}]_n$ (TM = Co, **(1)**; Ni, **(2)**), $[(Cu(bipy)_2)_2(C_6H_5PO_3)_2Mo_5O_{15}] \cdot 2H_2O$ (**(3)**) and $[(Zn(bipy)(\mu-OH))_2(Zn(bipy)_2(C_6H_5PO_3)_2Mo_5O_{15})_2] \cdot 3H_2O$ (**(4)**) (bipy = 2,2'-bipyridine), were successfully constructed under hydrothermal conditions, and their structures were determined by single crystal X-ray diffraction analysis and spectroscopic methods. The central heteroatoms in these polyoxometalates (POMs) are all organophosphine (RP) groups. Compound **1** and compound **2** are isostructural $(PhP)_2Mo_5$ -based TM-coordination polymers with the two-dimensional layer frameworks. In compound **3**, the bi-supporting structure containing one $(PhP)_2Mo_5$ unit and two $[Cu(bipy)_2]^{2+}$ cations. For compound **4**, it can be regarded as a dimer of two bi-supporting $\{Zn(bipy)_2(PhP)_2Mo_5Zn(bipy)\}$ clusters that were connected by two $\mu-OH$ groups. The acid-catalytic activities and fluorescence properties of the four hybrids have been investigated.

1. Introduction

Inorganic-organic hybrid materials based on polyoxometalates (POMs) have always been the focus of POM chemistry and the related subjects, which may be due to their diverse structures, special properties, and attractive applications in the fields of medicine, magnetic materials and catalytic materials [1–3]. Strandberg-type POMs, as one kind of small molecules in POM family, have been found to exhibit many excellent behaviors, such as high electron density, good stability and catalytic activity [4–6]. But they have not attracted enough attention by researchers compared with other types of POMs. The polyoxoanions of Strandberg-type POMs are capable of coordinating with transitional metal ions by octahedral and tetrahedral oxygen atoms, forming many fascinating structures [4,6b,7]. Especially, the centre inorganic phosphorus atoms of the polyoxoanion can be replaced by the organophosphine (RP) groups, and thus results in new inorganic-organic hybrid POMs. Zubieta's group has reported a series of Strandberg-type hybrid organophosphomolybdate compounds since 2001 [7a–b,8], and they investigated the magnetic properties of some compounds containing transition metal (TM) ions [7a–b,8c–f]. In these compounds, the centre RP groups include phosphonocarboxylate groups, alkylphosphonic acids, diphosphonic acids, etc. In recent years, Chen's group further researched the pentamolybdodiphosphates [9],

they obtained a new Strandberg anion with phosphonocarboxylate centre, in which the terminal carboxylate groups were firstly coordinated with TM ions [9b]. In 2016, Yang's group separated $(PhP)_2Mo_5$, $[Mo_7O_{24}]^{6-}$ and $[Mo_8O_{26}]^{4-}$ anions through capillary zone electrophoresis in the synthetic process of $(PhP)_2Mo_5$, and investigated the solution stability and equilibria of the three polyoxoanions, the results showed that the synthetic conditions of Strandberg-type POMs containing RP centre groups are relatively harsh comparing to $[P_2Mo_5O_{23}]^{6-}$ with the inorganic phosphorus centre [10]. This study perhaps provides valuable information for the synthesis of these POM compounds. Recently, our group successfully obtained two new Strandberg-type organophosphomolybdates and one organophosphotungstate modified by Cu-4,4'-bipyridine/H₂O complex units [6b–c], and further explored their acid-catalytic performances in the synthesis of cyclohexanone ethylene ketal. It is worth noting that the catalytic activities of RP-based compounds are higher than those with central inorganic phosphorus atoms [6a]. In addition, the three compounds displayed good photoluminescence property. As a continuation of our previous work, we wish to design and synthesize a series of new compounds containing $(PhP)_2Mo_5$ cluster and TM-bipy subunits through hydrothermal methods. In the present work, Co(II), Ni(II), Cu(II) and Zn(II)-bipy/H₂O complexes were successfully introduced into the skeletons of $(PhP)_2Mo_5$ polyoxoanions by controlling the

* Corresponding authors.

E-mail addresses: chemzhu@sina.com (Z.-M. Zhu), zhanglei@126.com (L.-C. Zhang).

<http://dx.doi.org/10.1016/j.jssc.2017.05.027>

Received 25 March 2017; Received in revised form 7 May 2017; Accepted 20 May 2017

Available online 21 May 2017

0022-4596/ © 2017 Elsevier Inc. All rights reserved.

reaction temperature, reaction time, pH and the ratio of starting materials, forming four new (PhP)₂Mo₅-based compounds, *i.e.* compounds **1–4**. Besides, the acid catalytic activities for the synthesis of cyclohexanone ethylene ketal and solid-state fluorescence properties of the four POMs have also been studied.

2. Experimental

2.1. Material and methods

All chemicals were of reagent grade as received from commercial sources and used without further purification. Elemental analyses were performed on a Vario El cube elemental analyzer for C, H, N, and a Prodigy XP emission spectrometer for P, Co, Ni, Cu, Zn and Mo. Single crystal X-ray diffraction data were collected on a Bruker Smart APEX II X-diffractometer equipped with graphite monochromated Mo K α radiation ($\lambda = 0.71073 \text{ \AA}$). The infrared spectra (IR) were recorded on KBr pellets with a Bruker AXS TENSOR-27 FTIR spectrometer in the range of 4000–400 cm⁻¹. The X-ray powder diffraction (XRPD) data were obtained on a Bruker AXS D8 Advance diffractometer using Cu K α radiation ($\lambda = 1.5418 \text{ \AA}$) with a step size of 0.02° in the 2 θ range from 5 to 60°. Thermogravimetric analysis (TGA) were carried out on a Pyris Diamond TG thermal analyzer in air at a heating rate of 10 °C min⁻¹. The solid UV spectra were recorded on a Agilent Cary-300 UV–visible spectrophotometer. The photoluminescence properties were determined on a Hitachi F-7000 fluorescence spectrophotometer in the solid state at room temperature. The yield of cyclohexanone ethylene ketal was confirmed on a JK-GC112A gas chromatograph.

2.2. Synthesis of compounds 1–4

2.2.1. Synthesis of compound [(Co(H₂O)(bipy))₂(C₆H₅PO₃)₂Mo₅O₁₅]_n (**1**)

C₆H₅PO₃H₂ (0.08 g, 0.5 mmol) and Na₂MoO₄·2H₂O (0.15 g, 0.6 mmol) were dissolved in 20 mL of distilled water under stirring at room temperature for 30 min. Then bipy (0.06 g, 0.4 mmol) was added to the above solution under stirring, and the pH of the mixture was adjusted to 3–4 with 4 mol L⁻¹ HCl, and CoCl₂·6H₂O (0.20 g, 0.8 mmol) was added simultaneously. The resulting mixture was transferred to a 30 mL Teflon-lined autoclave and kept at 150 °C for 3 days, and then brick red block crystals were obtained (yield: *ca.* 71% based on Mo). Elemental analysis calculated for C₃₂H₃₀O₂₃N₄Co₂P₂Mo₅: C 25.66, H 2.02, N 3.74, P 4.14, Co 7.87, Mo 32.03%; Found: C 25.70, H 2.05, N 3.65, P 4.08, Co 7.76, Mo 32.21%. IR (KBr pellet, ν/cm^{-1}): 3417 (m), 3065 (w), 2927 (w), 1605 (m), 1442 (m), 1317 (w), 1250 (w), 1147 (w), 1101 (s), 1055 (w), 977 (w), 937 (s), 904 (s), 694 (s), 597 (w), 551 (m).

2.2.2. Synthesis of compound [(Ni(H₂O)(bipy))₂(C₆H₅PO₃)₂Mo₅O₁₅]_n (**2**)

The detailed procedure for the preparation of compound **2** was similar to that of compound **1** except using NiCl₂·6H₂O (0.20 g, 0.8 mmol) instead of CoCl₂·6H₂O. Green block crystals of compound **2** in the yield of *ca.* 61% based on Mo were isolated from the filtrate. Elemental analysis calculated for C₃₂H₃₀O₂₃N₄Ni₂P₂Mo₅: C 25.66, H 2.02, N 3.74, P 4.14, Ni 7.84, Mo 32.04%; Found: C 25.71, H 2.11, N 3.68, P 4.09, Ni 7.92, Mo 31.92%. IR (KBr pellet, ν/cm^{-1}): 3325 (m), 3058 (w), 2927 (w), 1605 (m), 1442 (m), 1311 (w), 1251 (w), 1140 (w), 1107 (s), 1055 (m), 977 (m), 931 (s), 694 (s), 597 (w), 547 (m).

2.2.3. Synthesis of compound [(Cu(bipy))₂(C₆H₅PO₃)₂Mo₅O₁₅]_n·2H₂O (**3**)

The dosages of C₆H₅PO₃H₂ and Na₂MoO₄·2H₂O were the same as those of compound **1**. The amount of CuCl₂·2H₂O was decreased to 0.3 mmol (0.05 g), while the amount of bipy was increased from 0.4 to 0.5 mmol (0.08 g), after the above materials were added into 20 mL of

distilled water according to the order, the pH of the mixture was finally adjusted to 3–4 with 4 mol L⁻¹ HCl, and the reaction temperature was increased to 170 °C. Blue block crystals were isolated (yield: *ca.* 81% based on Mo). Elemental analysis calculated for C₅₂H₄₆O₂₃N₈Cu₂P₂Mo₅: C 34.32, H 2.55, N 6.16, P 3.40, Cu 6.98, Mo 26.37%, Found: C 34.40, H 2.58, N 6.25, P 3.35, Cu 6.91, Mo 26.28%. IR (KBr pellet, ν/cm^{-1}): 3452 (s), 3079 (m), 2927 (w), 1605 (m), 1442 (m), 1317 (w), 1251 (w), 1127 (m), 1042 (m), 977 (m), 904 (s), 773 (m), 694 (s), 564 (m).

2.2.4. Synthesis of compound [(Zn(bipy)(μ -OH))₂(Zn(bipy))₂(C₆H₅PO₃)₂Mo₅O₁₅]₂·3H₂O (**4**)

Compound **4** was synthesized in the same way as that of compound **3**, with the exception of the amount of C₆H₅PO₃H₂ (0.05 g, 0.3 mmol), ZnSO₄·7H₂O (0.10 g, 0.3 mmol) and bipy (0.05 g, 0.3 mmol), meanwhile the reaction time was changed to 4 days. Colorless transparent bulk crystals were obtained in *ca.* 13% yield (based on Mo). Elemental analysis calculated for C₈₄H₇₈O₄₇N₁₂Zn₄P₄Mo₁₀: C 30.10, H 2.35, N 5.01, P 3.70, Zn 7.80, Mo 28.62%, Found: C 30.02, H 2.40, N 5.09, P 3.62, Zn 7.92, Mo 28.53%. IR (KBr pellet, ν/cm^{-1}): 3440 (s), 3132 (m), 2925 (w), 1603 (m), 1442 (m), 1393 (m), 1317(w), 1247 (w), 1143 (w), 1101 (m), 983 (w), 906 (s), 697 (s), 544 (m).

2.3. Single crystal X-ray crystallography

The structures were solved by direct methods and refined by full-matrix least-squares fitting on F^2 using SHELXTL-97 [11,12]. An empirical absorption correction was applied using the SADABS program. Crystal data and structure refinement parameters of compounds **1–4** are listed in Table 1. In compounds **1–4**, H atoms on C atoms were added in calculated positions. The selected bond lengths and angles, and the hydrogen bonds are listed in Tables S1–S5. CCDC reference numbers: 1527719–1527722.

2.4. Catalytic experiment

According to the catalytic experimental method described in our previous work [6], the catalytic activities for the synthesis of cyclohexanone ethylene ketal of the title compounds were evaluated and compared to those of the parent compounds. The main procedures

Table 1
Crystal and refinement data for compounds **1–4**.

	1	2	3	4
Formula	C ₃₂ H ₃₀ O ₂₃ N ₄ Co ₂ P ₂ Mo ₅	C ₃₂ H ₃₀ O ₂₃ N ₄ Ni ₂ P ₂ Mo ₅	C ₅₂ H ₄₆ O ₂₃ N ₈ Cu ₂ P ₂ Mo ₅	C ₈₄ H ₇₈ O ₄₇ N ₁₂ Zn ₄ P ₄ Mo ₁₀
Formula weight	1498.10	1497.66	1819.69	3352.34
T/K	296(2)	296(2)	296(2)	296(2)
Wavelength/ \AA	0.71073	0.71073	0.71073	0.71073
Crystal system	Monoclinic	Monoclinic	Monoclinic	Monoclinic
Space group	C2/c	C2/c	C2/c	P21/n
$a/\text{\AA}$	17.441(5)	17.3800(15)	20.697(2)	11.790(2)
$b/\text{\AA}$	10.679(5)	10.8393(10)	12.8566(13)	22.631(4)
$c/\text{\AA}$	24.081(9)	24.017(2)	22.387(2)	20.095(3)
$\beta/^\circ$	97.998(9)	97.0220(10)	92.502(2)	101.971(3)
$V/\text{\AA}^3, Z$	4442(3), 4	4490.6(7), 4	5951.3(10), 4	5245.3(16), 2
$D_c/\text{g cm}^{-3}, F_{000}$	2.240, 2912	2.215, 2920	2.031, 3584	2.123, 3284
GOF	1.015	1.037	1.014	1.023
Reflections collected	11220	11255	15031	26734
Unique data, R_{int}	3920, 0.0390	3943, 0.0193	5238, 0.0248	9216, 0.0508
θ Range ($^\circ$)	1.71 to 25.00	1.71 to 25.00	1.82 to 25.00	1.80 to 25.00
$R_1(I > 2\sigma(I))^a$	0.0299	0.0200	0.0243	0.0426
wR_2 (all data) ^a	0.0614	0.0469	0.0561	0.0948

^a $R_1 = \sum ||F_o| - |F_c|| / \sum |F_o|$; $wR_2 = \sum [w(F_o^2 - F_c^2)^2] / \sum [w(F_o^2)]^{1/2}$

are as follows: the catalyst was added to a mixture of cyclohexanone and glycol, and 10 mL of cyclohexane was used as a water-carrying agent in the reaction process. After completing the reaction, the heterogeneous catalyst could be easily separated from the reaction mixture through decantation or filtration, and washed and dried, and then used directly for the next reaction cycle. The reusability of the catalysts were investigated under the optimum reaction conditions.

3. Results and discussion

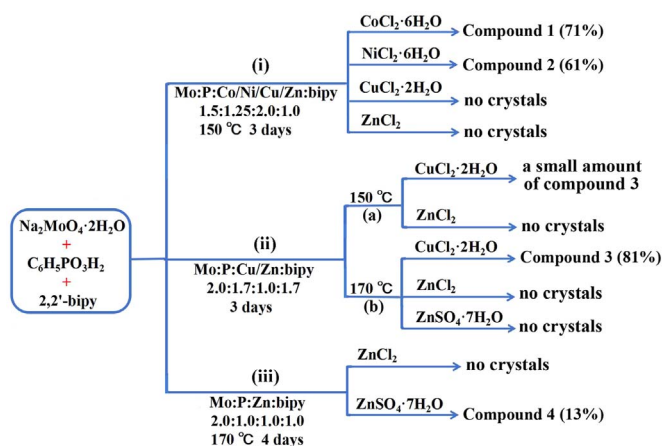
3.1. Synthesis

RP groups can be introduced into the interior of the Strandberg-type POM skeleton, forming very interesting inorganic-organic hybrid compounds, e.g. (RP)₂Mo₅ and (RP)₂W₅-based compounds. However, these kinds of compounds are usually difficult to obtain because their synthetic conditions including reaction temperature, molar ratio and adding order of raw materials, pH, etc. are very harsh. In order to synthesize this sort of compounds, Na₂MoO₄·2H₂O, C₆H₅PO₃H₂ and bipy as well as different TMs (Co(II), Ni(II), Cu(II) or Zn(II)) were used as the starting materials. Based on our recent work [6b], the synthetic methods of these compounds were designed, and the synthetic pathways are illustrated in Scheme 1. By groping various experiment conditions, two new crystalline (PhP)₂Mo₅-based coordination polymers (isostructural compound **1** and compound **2**) containing Co(II) and Ni(II)-bipy/H₂O complexes were finally obtained with the molar ratio of Mo: P: TM: bipy being 1.5: 1.25: 2.0: 1.0 at 150 °C after 3 days. However, no crystals of Cu(II) or Zn(II)-based compounds were obtained under the same conditions (Scheme 1(i)). Therefore, the synthetic and crystallization conditions of this type of POMs varied with different TMs. When changing the molar ratio of Mo: P: Cu: bipy to 2.0: 1.7: 1.0: 1.7 and other conditions remain unchanged, only a small amount of impure crystals of Cu(II)-(PhP)₂Mo₅ complex (compound **3**) were generated (Scheme 1(ii)a). In pathway (ii), when increasing the temperature to 170 °C, crystalline compound **3** with 81% yield was achieved successfully (Scheme 1(ii)b), which means the higher temperature is critical to obtain a relatively pure compound with high yield. Unfortunately, still no Zn(II)-based crystals were obtained under the identical conditions. To obtain Zn(II)-(PhP)₂Mo₅ complex, large amounts of experiments were carried out. The experimental results showed that when the molar ratio of Mo: P: Zn: bipy was adjusted to 2.0: 1.0: 1.0: 1.0, and the reaction time was further increased to 4 days at 170 °C, pure crystalline compound **4** can be got (Scheme 1(iii)). But the product yield needs to be further increased, and the optimum conditions need further improving. As can be seen from Scheme 1(iii), remarkably, if using ZnCl₂ instead of ZnSO₄·7H₂O

and keeping other conditions unchanged, no crystals were obtained. Interestingly, the adding order of TMs has a significant effect on the formation and crystallization of the compounds. TM should be added after adjusting the pH for the synthesis of compound **1** or **2**, while for the synthesis of compound **3** or **4**, TM must be added before adjusting the pH. In addition, the pH also plays a key role in the synthesis of these Strandberg-type POMs with RP. The range of pH from 3 to 4 is suitable for acquiring reasonable yields of these crystalline compounds.

3.2. Structural analysis

Single crystal X-ray diffraction analysis reveals that compounds **1** and **2** are isostructural tetra-supporting POM-based inorganic-organic hybrids. Compound **1/2** is considered as a Co(II)/Ni(II) coordination polymer, which consists of (PhP)₂Mo₅ polyanions and [Co/Ni(H₂O)(bipy)]²⁺ cations (Fig. 1a, Fig. S1a and Fig. S1b). As shown in Fig. 1a, the (PhP)₂Mo₅ unit acts as a hexadentate ligand, connecting four Co(II)/Ni(II) ions via four terminal oxygen atoms (O5, O5', O9, O9') and two bridging oxygen atoms (O1, O1'). Co1/Ni1 coordinates with two N atoms (N1, N2) from one bipy ligand, and two terminal oxygen atoms (O5, O9) and one bridge oxygen atoms (O1) of the polyoxoanion, and one terminal water ligand (O1W). The bond lengths of Co–O/OW and Co–N are 2.042 (3)–2.206 (3) and 2.078 (4)–2.086 (4) Å, respectively. The bond lengths of Ni–O/OW and Ni–N are 2.0311 (18)–2.1596 (19) and 2.032 (2)–2.038 (2) Å, respectively. The Mo–O distances are in the range of 1.678 (3)–2.410 (3) and 1.690 (2)–2.4203 (18) Å for **1** and **2**, respectively (Tables S1 and S2). As shown in Fig. 1b, the adjacent two (PhP)₂Mo₅ units are linked by a Co(II)/Ni(II) ion, and each (PhP)₂Mo₅ is surrounded by six (PhP)₂Mo₅ units, forming a plane, and the adjacent planes are parallel to each other to further form a 3-D framework through hydrogen bonding interactions (Fig. 1c). The hydrogen bonds of O–H...O are 2.706(4)–2.772(4) Å and 2.708(2)–2.761(2) Å for **1** and **2**, respectively (Table 5). The 2-D network topology of compound **1/2** can be further described as in Fig. 2b. In this simplification, the (PhP)₂Mo₅ unit act as one kind of four-node, the Co(II)/Ni(II)-bipy subunit is simplified into a straight line (Fig. 2a). From the topological point of view, the 2-D structure of compound **1/2** can be simplified to a unique four-connected 4-c net with stoichiometry (4-c), and the point symbol for the net is (4⁴·6²). In compound **3**, as we can see from Fig. 3 and S2a, each molecule contains one (PhP)₂Mo₅ unit, two [Cu(bipy)₂]²⁺ and two lattice water molecules, in which two [Cu(bipy)₂]²⁺ fragments support on the two sides of Strandberg-type anion through two terminal oxygen atoms of MoO₆ octahedra, forming a bi-supporting structure. All Cu(II) ions adopt five-coordinated square-pyramidal coordination geometries, and the Cu1–O10 bond length is 2.065 (3) Å, and the bond lengths of Cu–N are 1.957 (4)–2.119 (5) Å. The Mo–O distances are in the range of 1.682 (3)–2.518 (3) Å (Table S3). A 3-D architecture is also constructed through hydrogen bonding and electrostatic interactions (Fig. S3). Compound **4**, as a dimer of (PhP)₂Mo₅, contains both the mononuclear and binuclear zinc complex units, and three lattice water molecules. As viewed from Fig. 4 and S2b, two bi-supporting {Zn(bipy)₂(PhP)₂Mo₅Zn(bipy)} clusters are bridged by two μ-OH groups coordinating with two Zn²⁺ ions of the {Zn(bipy)} units, it also can be regarded as two mono-supporting {Zn(bipy)₂(PhP)₂Mo₅} clusters are linked by a binuclear zinc complex [Zn(bipy)(μ-OH)₂Zn(bipy)] through four oxygen atoms of the two polyoxoanions, forming a symmetrical structure. In the single crystal structure of compound **4**, Zn(II) ions exists in two different coordination environments, the asymmetric Zn1 is hexa-coordinated by four nitrogen atoms (N1, N2, N3, N4) from two bipy molecules (Zn–N, 2.080(6)–2.168(5) Å), one terminal oxygen atom (O5) from a MoO₆ octahedron group (Zn–O5 2.240(4) Å), and one bridge oxygen atom (O4) from corner-sharing MoO₆ octahedron group and PO₄ tetrahedron (Zn–O4 2.108(4) Å), forming ZnN₄O₂ octahedron. Zn2 centre is also in an octahedral coordination environment, it coordinates with two nitrogen atoms (N5, N6) from one bipy molecule, one terminal oxygen atom (O21) from a MoO₆ octahedron, one bridge oxygen atom (O16) from corner-sharing MoO₆ octahedron and



Scheme 1. Schematic representation of the synthetic pathways and conditions of compounds **1–4**.

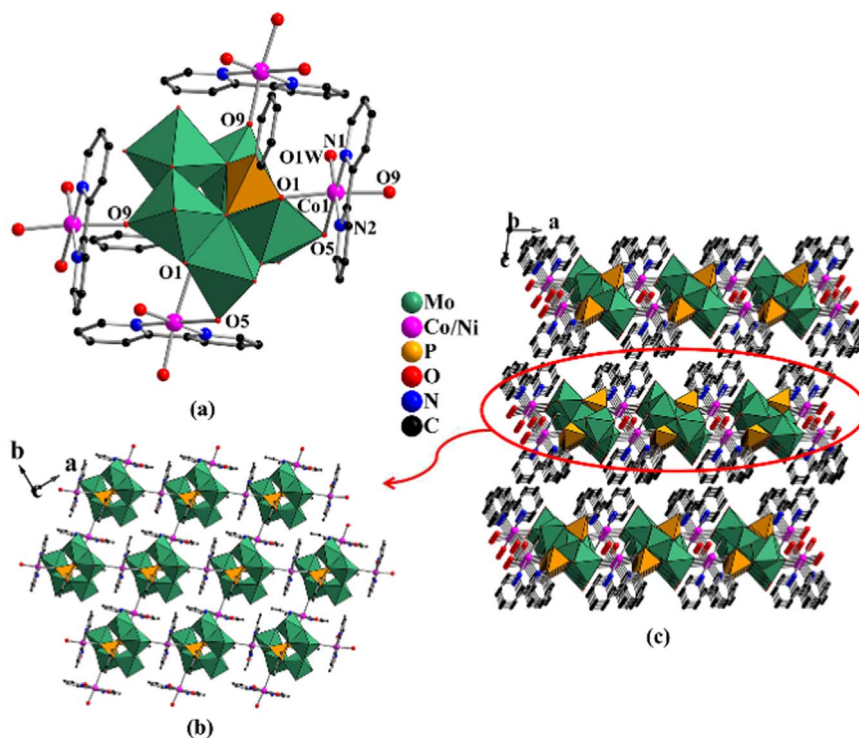


Fig. 1. (a) Structural representation of the coordination environment of four Co(II)/Ni(II) ions coordinating with the $(\text{PhP})_2\text{Mo}_5$ cluster in compound **1/2**; (b) The infinite 2-D layers of compound **1/2**; (c) The packing view of the infinite 3-D network for **1/2**.

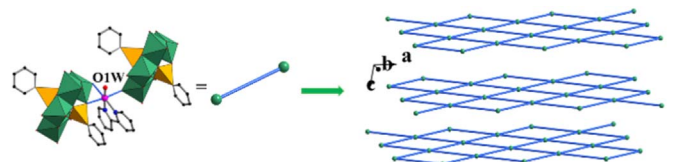


Fig. 2. (a) Perspective views of the connected (Co(II)/Ni(II) ions and $(\text{RP})_2\text{Mo}_5$ polyanion) nodes in compound **1/2**; (b) the topology framework of **1/2** with (4^1-6^2) .

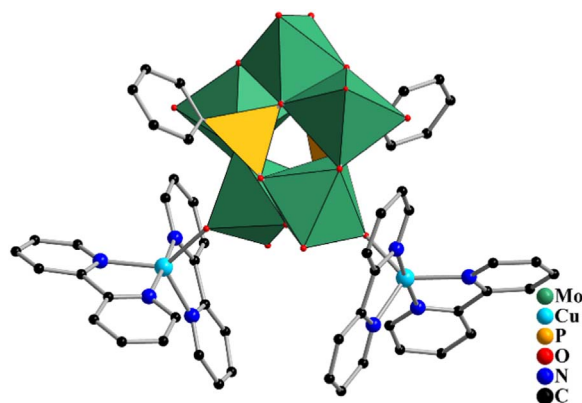


Fig. 3. Combined polyhedral and ball-and-stick representation for compound **3**.

PO_4 tetrahedron, and two bridge oxygen atoms (O22 and O22') of two μ -OH groups, forming $\text{Zn}_2\text{N}_2\text{O}_4$ octahedron. The bond lengths of Zn2–N5, Zn2–N6, Zn2–O16, Zn2–O21 and Zn–O22/O22' are 2.085(6), 2.080(6), 2.062(4), 2.194(5) and 2.209(5) Å, respectively. The Mo–O distances are in the range of 1.685(4)–2.481(4) Å (Table S4). Fig. S4 exhibits a 3-D stacked graph of compound **4** formed by the hydrogen bonding and electrostatic interactions.

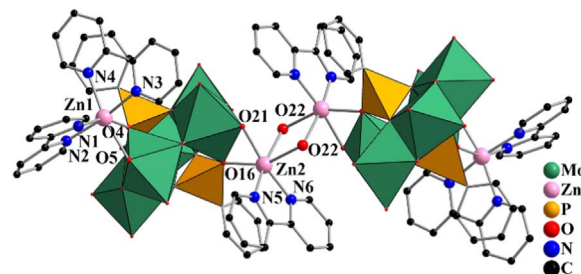


Fig. 4. Combined polyhedral and ball-and-stick representation for compound **4**.

3.3. IR spectra of compounds 1–4

The bands in the IR of compounds 1–4 (Fig. S5) at 3452–2925 cm^{-1} are attributed to the characteristic vibrations of O–H and C–H. The bands in the region of 1605–1247 cm^{-1} are associated with the pyridine ring of a bipy molecule [6b–c]. The bands of 1147–1042 cm^{-1} are due to the $\nu(\text{P–O})$ of the organophosphonate ligands, and bands at 983–977, 937–694 cm^{-1} belong to $\nu(\text{Mo–O}_{\text{terminal}})$ and $\nu(\text{Mo–O}_{\text{bridging}})$ of polyoxoanion, respectively [9].

3.4. XRPD

The XRPD of the crystalline samples were tested at room temperature in order to evaluate the purity of as-synthesized compounds. As shown in Fig. S6, all major peaks of the simulated and experimental XRPD patterns are in agreement with each other, indicating their reasonable crystalline phase purity for compounds 1–4. The differences in intensity may be due to the preferred orientation of the crystalline powder samples.

3.5. TGA

The thermal behaviors of compounds **1–4** were investigated with the thermal analysis methods, and their TGA curves are given in Fig. S7. It is found that the four compounds all display a three-continuous weight loss. As shown in Fig. S7a and Fig. S7b, in the temperature range of 30–650 °C, the total weight losses of 32.94% and 33.02% for compound **1** and compound **2** respectively are due to the removal of two coordinate water molecules, two bipy molecules and two phenyl groups, which are consistent with the calculated values (calcd. 33.55% and 33.57%). For compound **3**, the total weight loss of 44.94% (calcd. 44.79%) in the temperature range of 30–640 °C corresponds to the loss of two crystalline water molecules, four bipy molecules and two phenyl groups (Fig. S7c). The TG curve of compound **4** exhibits the total weight loss of 40.38% (calcd. 39.84%) at 30–550 °C, which matches to the loss of three crystalline water molecules, six bipy molecules, four phenyl groups and two μ -OH groups (Fig. S7d).

3.6. Solid UV–vis absorption and fluorescence spectra

In order to further understand the optical properties of the four compounds, the diffuse reflectivity spectra in absorption mode of the parent $(\text{NH}_4)_4[(\text{C}_6\text{H}_5\text{PO}_3)_2\text{Mo}_5\text{O}_{15}]$ ($(\text{NH}_4)(\text{PhP})_2\text{Mo}_5$), bipy and compounds **1–4** from 200 to 800 nm are presented in Fig. S8. As seen from Fig. S8, the parent $(\text{NH}_4)(\text{PhP})_2\text{Mo}_5$ has a strong band (292 nm) ($\text{O} \rightarrow \text{Mo}$) only in the UV region [13]. The absorption at 216 and 260 nm of bipy in the UV region is ascribed to the $\pi \rightarrow \pi^*$ transition [14]. While the four title inorganic–organic hybrid compounds show the strong bands (302, 308, 305, 310 nm) in the UV and visible region (505, 619, 764 nm). Consequently, the absorption bands in the UV range of compounds **1–4** were assigned to a charge-transfer transition from the ligand to metal (LMCT) of $\text{O} \rightarrow \text{Mo}$ and the characteristic absorption of bipy [6a], while the absorption at 500–800 nm are due to the d–d transition coming from the introduction of TM ($\text{Co(II)/Ni(II)/Cu(II)}$) ions.

The luminescence properties of compounds **1–4** and the parent $(\text{NH}_4)(\text{PhP})_2\text{Mo}_5$ in the solid state at room temperature are depicted in Fig. S9. As shown in Fig. S9, the parent $(\text{NH}_4)(\text{PhP})_2\text{Mo}_5$ displays luminescence with two main emission peaks at 398 and 470 nm with $\lambda_{\text{ex}} = 305$ nm, which should be assigned to ligand-to-metal charge transfer (LMCT, $\text{O} \rightarrow \text{Mo}$) [9]. Compounds **1–4** all show emission peaks at 398 and 470 nm ($\lambda_{\text{ex}} = 305$ nm), indicating that they have a similar structure. Compared with the emission of the parent $(\text{NH}_4)(\text{PhP})_2\text{Mo}_5$, emissions of compounds **1–4** are mainly caused by the $(\text{PhP})_2\text{Mo}_5$ cluster, furthermore, the emission intensities of compounds **1–4** have changed, that is, the coordination of $(\text{PhP})_2\text{Mo}_5$ to $\text{Co(II)/Ni(II)/Cu(II)/Zn(II)}$ ions quenches partially LMCT ($\text{O} \rightarrow \text{Mo}$). The emission peaks at about 390 nm and 409 nm for bipy and 293 nm for $\text{C}_6\text{H}_5\text{PO}_3\text{H}_2$ ($\lambda_{\text{ex}} = 305$ nm) should be assigned to $\pi^* \rightarrow \pi$ transition [6b–c].

3.7. Catalytic activities of compounds 1–4

The title compounds were applied as catalysts in the synthesis of cyclohexanone ethylene ketal (Scheme S1) [6b–c,15]. In order to investigate the optimal catalytic reaction conditions for the four compounds, the effects of various factors including reaction time, the amount of catalyst and molar ratio of cyclohexanone to glycol were systematically investigated and selected. Taking compound **1** as an example, the catalytic performances are shown in Figs. S10–S12, and the optimum conditions for the synthesis of cyclohexanone ethylene ketal were as follows: (1) the reaction time was 4.0 h, reaction temperature was 95–100 °C and 10 mL of a cyclohexane water-carrying agent; (2) the molar ratio of cyclohexanone and glycol was 1:1.4; (3) the molar ratio of the catalyst to cyclohexanone was 1:200. Under the optimum conditions, the acid-catalytic activities of com-

Table 2

Catalytic performances of **1–4** compared with the reference catalysts for the synthesis of cyclohexanone ethylene ketal.

Entry	Catalyst	Solubility	Time (h)	Yield (%)
1	Compound 1	Insoluble	4.0	90
2	Compound 2	Insoluble	4.0	88
3	Compound 3	Insoluble	4.0	89
4	Compound 4	Insoluble	4.0	89
5	$\text{NH}_4(\text{PhP})_2\text{Mo}_5$ [13]	Insoluble	4.0	81
6	4,4'-bipy-Cu-(PhP) $_2\text{Mo}_5$ [6b]	Insoluble	2.5	91
7	$\text{CoCl}_2 \cdot 6\text{H}_2\text{O}$	soluble	4.0	98
8	$\text{NiCl}_2 \cdot 6\text{H}_2\text{O}$	soluble	4.0	98
9	$\text{CuCl}_2 \cdot 2\text{H}_2\text{O}$	soluble	4.0	99
10	$\text{ZnSO}_4 \cdot 7\text{H}_2\text{O}$	soluble	4.0	98
11	–	–	4.0	10

Reaction conditions: the molar ratio of cyclohexanone to glycol was 1:1.4 (0.1 mol of cyclohexanone); water-carrying agent: 10 mL of cyclohexane; reaction temperature: 95–100 °C. The molar ratio of the catalyst to cyclohexanone is 1:200. 4,4'-bipy-Cu-(PhP) $_2\text{Mo}_5 = [(\text{Cu}(\text{H}_2\text{O})_2)_2(\mu\text{-bipy})(\text{C}_6\text{H}_5\text{PO}_3)_2\text{Mo}_5\text{O}_{15}]_n$

pounds **1–4**, the parent $(\text{NH}_4)(\text{PhP})_2\text{Mo}_5$ and metal salts are listed in Table 2. As seen from Table 2, compared with the parent $(\text{NH}_4)(\text{PhP})_2\text{Mo}_5$, the yields of ketal for compounds **1–4** are all increased. It is also found that their catalytic activity approaches that of $[(\text{Cu}(\text{H}_2\text{O})_2)_2(\mu\text{-bipy})(\text{C}_6\text{H}_5\text{PO}_3)_2\text{Mo}_5\text{O}_{15}]_n$ reported previously by our group [6b]. While in the absence of catalyst, the yield of ketal is very low (10%), which shows that the title compounds display higher acid-catalytic activities. In addition, the inorganic salts, $\text{CoCl}_2 \cdot 6\text{H}_2\text{O}$, $\text{NiCl}_2 \cdot 6\text{H}_2\text{O}$, $\text{CuCl}_2 \cdot 2\text{H}_2\text{O}$ and $\text{ZnSO}_4 \cdot 7\text{H}_2\text{O}$, exhibit high catalytic activity, but they act as the homogeneous catalysts, which were not able to be recycled. From the above analysis, it can be inferred that $\text{Co(II)/Ni(II)/Cu(II)/Zn(II)}$ ions as well as Mo(VI) moieties as the catalytically active centres, playing important roles in the catalytic reaction [6b]. Moreover, the reusability of the title compounds was also examined (Fig. 5). As shown in Fig. 5, we found that they maintained the catalytic activities after being reused for 3 times, the reason for the slight decrease in catalytic yield may be the loss of some catalyst during the washing process with ether. To further confirm the stability of these compounds after the catalytic reactions, the catalysts before and after used four runs were characterized by IR and XRPD (Figs. S13 and S14). As shown in Fig. S13, the IR characteristic peaks of the powder samples after the catalysis are consistent with those of crystalline compounds **1–4** before the catalysis. As shown in Fig. S14, the main diffraction peaks positions are consistent with the simulated values of compounds **1–4**, and the different intensity of peaks may be caused by the diverse preferred orientation of the powder samples. These results indicate that the structures of compounds **1–4** are intact after the catalytic process. Based on the above results, it is concluded that

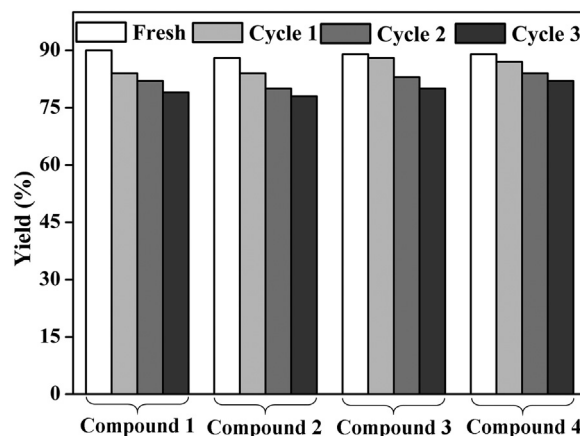


Fig. 5. The catalytic activities of compounds **1–4** reused for three cycles.

compounds **1–4** are stable and can be used as efficient heterogeneous acid catalysts for the synthesis of cyclohexanone ethylene ketal.

4. Conclusion

In summary, four inorganic-organic hybrids based on $(\text{PhP})_2\text{Mo}_5$ clusters and $\text{Co(II)/Ni(II)/Cu(II)/Zn(II)-(bipy)/H}_2\text{O}$ units enriches the structural diversity of the Strandberg-type POMs with organophosphine centres. Many factors, such as the pH, reaction temperature, reaction time, and adding order and proportion of the starting materials are all very important for the formation and crystallization of them, which also show that their synthetic conditions are very harsh. Compared with their parent $\text{NH}_4\text{-(PhP)}_2\text{Mo}_5$, the title compounds exhibit better acid catalytic activities and can be easily recovered and reused on the synthesis of cyclohexanone ethylene ketal. Further research on other organophosphomolybdates is underway in our group.

Acknowledgements

This work was financially supported by the National Natural Science Foundation of China (nos. 21671091 and 21503103); the Youth scientific research project of Liaoning Normal University (nos. LS2014L018 and LS2015L008).

Appendix A. Supplementary material

Supplementary data associated with this article can be found in the online version at doi:10.1016/j.jssc.2017.05.027.

References

- [1] (a) C. Dey, T. Kundu, R. Banerjee, *Chem. Commun.* 48 (2012) 266–268; (b) J.T. Rhule, C.L. Hill, D.A. Judd, R.F. Schinazi, *Chem. Rev.* 98 (1998) 327–358.
- [2] (a) S. Cardona-Serra, J.M. Clemente-Juan, E. Coronado, A. Gaita-Ariño, A. Camón, M. Evangelisti, F. Luis, M.J. Martínez-Pérez, J. Sesé, *J. Am. Chem. Soc.* 134 (2012) 14982–14990; (b) J.M. Maestre, X. Lopez, C. Bo, J.M. Poblet, N. Casañ-Pastor, *J. Am. Chem. Soc.* 123 (2001) 3749–3758.
- [3] (a) H.J. Lv, Y.V. Geletii, C.C. Zhao, J.W. Vickers, G.B. Zhu, Z. Luo, J. Song, T.Q. Lian, D.G. Musaev, C.L. Hill, *Chem. Soc. Rev.* 41 (2012) 7572–7589; (b) A.M. Khenkin, I. Efrementko, J.M.L. Martin, R. Neumann, *J. Am. Chem. Soc.* 135 (2013) 19304–19310; (c) J.J. Stracke, R.G. Finke, *ACS Catal.* 4 (2014) 79–89; (d) Y. Yang, B. Zhang, Y.Z. Wang, L. Yue, W. Li, L.X. Wu, *J. Am. Chem. Soc.* 135 (2013) 14500–14503; (e) C. Zou, Z.J. Zhang, X. Xu, Q.H. Gong, J. Li, C.D. Wu, *J. Am. Chem. Soc.* 134 (2012) 87–90; (f) J.P. Bai, F. Su, H.T. Zhu, H. Sun, L.C. Zhang, M.Y. Liu, W.S. You, Z.M. Zhu, *Dalton Trans.* 44 (2015) 6423–6430;
- (g) H. Sun, L.Y. Guo, J.S. Li, J.P. Bai, F. Su, L.C. Zhang, X.J. Sang, W.S. You, Z.M. Zhu, *ChemSusChem* 9 (2016) 1125–1133;
- (h) R. Kawahara, R. Osuga, J.N. Kondo, N. Mizuno, S. Uchida, *Dalton Trans.* 46 (2017) 3105–3109;
- (i) Y.L. Ren, L. Li, B. Mu, C.X. Li, R.D. Huang, *J. Solid State Chem.* 249 (2017) 1–8;
- (j) X.X. Lu, Y.H. Luo, C. Lu, X. Chen, H. Zhang, *J. Solid State Chem.* 232 (2015) 123–130.
- [4] K. Yu, B.B. Zhou, Y. Yu, Z.H. Su, H.Y. Wang, C.M. Wang, C.X. Wang, *Dalton Trans.* 41 (2012) 10014–10020.
- [5] C. Qin, X.L. Wang, L. Yuan, E.B. Wang, *Cryst. Growth Des.* 8 (2008) 2093–2095.
- [6] (a) Z.L. Li, Y. Wang, L.C. Zhang, J.P. Wang, W.S. You, Z.M. Zhu, *Dalton Trans.* 43 (2014) 5840–5846; (b) J.P. Wang, H.X. Ma, L.C. Zhang, W.S. You, Z.M. Zhu, *Dalton Trans.* 43 (2014) 17172–17176; (c) H.X. Ma, J. Du, Z.M. Zhu, T. Lu, F. Su, L.C. Zhang, *Dalton Trans.* 45 (2016) 1631–1637.
- [7] (a) N.G. Armatas, D.G. Allis, A. Prosvirin, G. Carnuti, C.J. O'Connor, K. Dunbar, J. Zubieta, *Inorg. Chem.* 47 (2008) 832–854; (b) T.M. Smith, K. Perkins, D. Symester, S.R. Freund, J. Vargas, L. Spinu, J. Zubieta, *CrystEngComm* 16 (2014) 191–213; (c) H.J. Jin, B.B. Zhou, Y. Yu, Z.F. Zhao, Z.H. Su, *CrystEngComm* 13 (2011) 585–590.
- [8] (a) R.C. Finn, J. Zubieta, *Inorg. Chem.* 40 (2001) 2466–2467; (b) R.C. Finn, R.S. Rarig Jr., J. Zubieta, *Inorg. Chem.* 41 (2002) 2109–2123; (c) E. Burkholder, V. Golub, C.J. O'Connor, J. Zubieta, *Inorg. Chem.* 42 (2003) 6729–6740; (d) E. Burkholder, V. Golub, C.J. O'Connor, J. Zubieta, *Inorg. Chem.* 43 (2004) 7014–7029; (e) N.G. Armatas, W. Ouellette, K. Whitenack, J. Pelcher, H.X. Liu, E. Romaine, C.J. O'Connor, J. Zubieta, *Inorg. Chem.* 48 (2009) 8897–8910; (f) P. DeBurgomaster, A. Aldous, H.X. Liu, C.J. O'Connor, J. Zubieta, *Cryst. Growth Des.* 10 (2010) 2209–2218.
- [9] (a) X.M. Li, Y.G. Chen, C.N. Su, S. Zhou, Q. Tang, T. Shi, *Inorg. Chem.* 52 (2013) 11422–11427; (b) X.M. Li, Y.G. Chen, T. Shi, S. Zhou, Q. Tang, *Inorg. Chem. Commun.* 50 (2014) 70–74.
- [10] S.C. Sun, X. Liu, L. Yang, H.Q. Tan, E.B. Wang, *Eur. J. Inorg. Chem.* 2016 (2016) 4179–4184.
- [11] G.M. Sheldrick, SHELXL97, Program for Crystal Structure Refinement, University of Göttingen, Germany, 1997.
- [12] G.M. Sheldrick, SHELXL97, Program for Crystal Structure Solution, University of Göttingen, Germany, 1997.
- [13] W.S. Kwak, M.T. Pope, P.R. Sethuraman, *Inorg. Synth.* 27 (1990) 125.
- [14] (a) N.M. Karayannis, *Coord. Chem. Rev.* 20 (1976) 37–80; (b) S. Sprouse, K.A. King, P.J. Spellane, R.J. Watts, *J. Am. Chem. Soc.* 106 (1984) 6647–6653.
- [15] J.H. Liu, X.F. Wei, Y.L. Yu, J.L. Song, X. Wang, A. Li, X.W. Liu, W.Q. Deng, *Chem. Commun.* 46 (2010) 1670–1672.